IL-34 Downregulation–Associated M1/M2 Macrophage Imbalance Is Related to Inflammaging in Sun-Exposed Human Skin

Satoshi Horiba[1], Ryota Kami[1], Taiki Tsutsui[1] and Junichi Hosoi[1]

Macrophages can be polarized into two subsets: a proinflammatory (M1) or an anti-inflammatory (M2) phenotype. In this study, we show that an increased M1-to-M2 ratio associated with a decrease in IL-34 induces skin inflammaging. The total number of macrophages in the dermis did not change, but the number of M2 macrophages was significantly decreased. Thus, the M1-to-M2 ratio was significantly increased in sun-exposed aged skin and positively correlated with the percentage of $p21^+$ and $p16^+$ senescent cells in the dermis. The supernatant of M1 macrophages increased the percentages of senescence-associated β-galactosidase–positive cells, whereas the supernatant of M2 macrophages decreased the percentages of senescence-associated β-galactosidase–positive cells in vitro. Among the mechanisms that could explain the increase in the M1-to-M2 ratio, we found that the number of $IL-34^+$ cells was decreased in aged skin and negatively correlated with the M1-to-M2 ratio. Furthermore, IL-34 induced the expression of CD206 and IL-10, which are M2 macrophage markers, in an in vitro assay. Our results suggest that a reduction in epidermal IL-34 in aged skin may skew the M1/M2 balance in the dermis and lead to low-grade chronic inflammation and inflammaging.

INTRODUCTION

In the skin, the immune system has distinct spatial and functional organization and maintains homeostasis (Tsepkolenko et al., 2019). In the dermis, various cells from the circulation accumulate and become activated. Dendritic cells form clusters with effector T cells in dermal perivascular areas, and these dermal leukocyte clusters are essential for eliciting acquired cutaneous immunity (Natsuaki et al., 2014). In addition, apoptotic T cells trigger macrophage activation, leading to increases in regulatory T cells and immune tolerance (Akiyama et al., 2012).

Among immune cells in the skin, dermal macrophages have well-documented roles (Mowat et al., 2017; Yanez et al., 2017), especially in wound healing (Lucas et al., 2010; Shook et al., 2018). Macrophages can roughly be divided into two subsets: M1 (proinflammatory) and M2 (anti-inflammatory) (Martinez and Gordon, 2014). Previous reports have shown that the balance between these two phenotypes is important for tissue homeostasis, repair, regeneration, and various diseases (Eapen et al., 2017; Mescher, 2017; Wynn and Vannella, 2016). However, the effect of aging on the M1/M2 balance in human skin is poorly understood.

Skin aging induced by the UV component of sunlight is called photoaging and is superimposed on chronological aging (Fisher et al., 2002; Gordon and Brieva, 2012). Photoaging is characterized by reduced production and increased fragmentation of the dermal extracellular matrix (Rittié and Fisher, 2015). In addition, exposure to UVB induces premature senescence in human dermal fibroblasts, causing photoaging in the dermis (Chen et al., 2008). Therefore, many studies have addressed the mechanism of aging in sun-exposed skin by investigating the components of the dermis, especially dermal fibroblasts (Qin et al., 2014; Yoshida and Okada, 2019). Senescent dermal fibroblasts express high levels of senescence-associated β-galactosidases (SA-β-gals), p16 and p21, which are senescence-specific markers (Idda et al., 2020; Ressler et al., 2006; van Deursen, 2014). The accumulation of senescent dermal fibroblasts that are positive for these markers diminishes the ability of the skin to resolve and repair inflammation and alters the phenotype and activity of immune cells, which can lead to a type of chronic low-level inflammation associated with aging known as inflammaging (Pilkington et al., 2021). However, the relationship between aging and the M1/M2 balance in sun-exposed skin has not been fully investigated.

In this study, we found a significant increase in the M1-to-M2 ratio in sun-exposed skin that was associated with accelerated inflammaging. We also observed a significant reduction in epidermal IL-34, which may induce an inflammatory environment and skew the M1/M2 balance in the dermis.

RESULTS

M1/M2 balance is skewed in sun-exposed aged skin

To determine aging-related changes in dermal macrophage phenotypes in sun-exposed skin, we stained human skin tissue samples for CD86, a human M1 macrophage surface marker; CD206, a human M2 macrophage surface marker;

[1]Shiseido Global Innovation Center, Yokohama, Japan

Correspondence: Satoshi Horiba, Shiseido Global Innovation Center, 1-2-11, Takashima, Nishi-ku, Yokohama 220-0011, Japan. E-mail: satoshi.horiba@shiseido.com

Abbreviation: SA-β-gal, senescence-associated β-galactosidase

Cite this article as: JID Innovations 2022;2:100112

Figure 1. The M1-to-M2 ratio is increased in aged skin. (**a**) Representative CD86 (green) and CD68 (red) immunofluorescence-stained samples of young (mean age = 34.2 years) and old (mean age = 74.5 years) human skin. The arrows indicate CD86$^+$ CD68$^+$ cells in the dermis. (**b**) Representative CD206 (green) and CD68 (red) immunofluorescence-stained samples of young and old human skin. The arrows indicate CD206$^+$ CD68$^+$ cells in the dermis. (**c**) Representative CD11b (green) and CD68 (red) immunofluorescence-stained samples of young and old human skin. The arrows indicate CD11b$^+$ CD68$^+$ cells in the dermis. (**d**) Quantitation of CD86$^+$ CD68$^+$ cells/mm^2 in the dermis. (**e**) Quantitation of CD206$^+$ CD68$^+$ cells/mm^2 in the dermis. (**f**) Quantitation of CD11b$^+$ CD68$^+$ cells/mm^2 in the dermis. (**g**) Quantitation of the M1/M2 ratio (number of CD86$^+$ CD68$^+$ cells/number of CD206$^+$ CD68$^+$ cells) in the dermis. Nuclei were stained with Hoechst (blue). All data are expressed as mean ± SD values. n = 10 in both the young and old groups. *$P < 0.05$ and **$P < 0.01$. To test for significance, the Mann–Whitney U test was utilized. Bar = 100 μm. n.s., not significant.
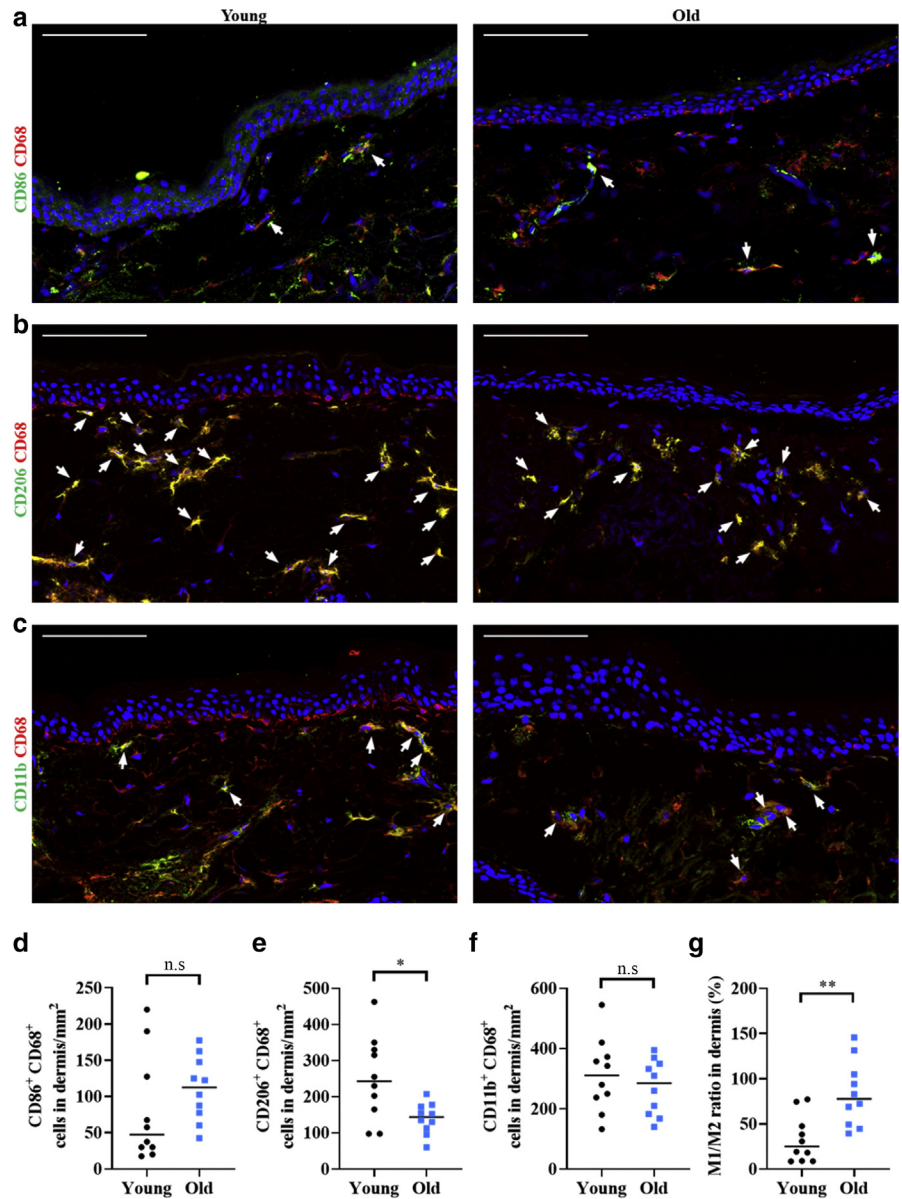
and CD68 and CD11b, which are human macrophage surface markers. The total number of macrophages (CD68$^+$ CD11b$^+$ cells) did not show a significant difference between young and aged skin (Figure 1c and f). However, the number of M2 macrophages (CD206$^+$ CD68$^+$ cells) was significantly decreased in aged skin ($P = 0.0224$, Mann–Whitney U test; Figure 1b and e). Although the difference was not significant, the number of M1 macrophages (CD86$^+$ CD68$^+$ cells) was increased in aged skin (Figure 1a and d), and the M1-to-M2 ratio in the dermis was significantly increased ($P = 0.0029$, Mann–Whitney U test; Figure 1g), indicating that the M1 and M2 macrophage balance was altered in sun-exposed aged skin.
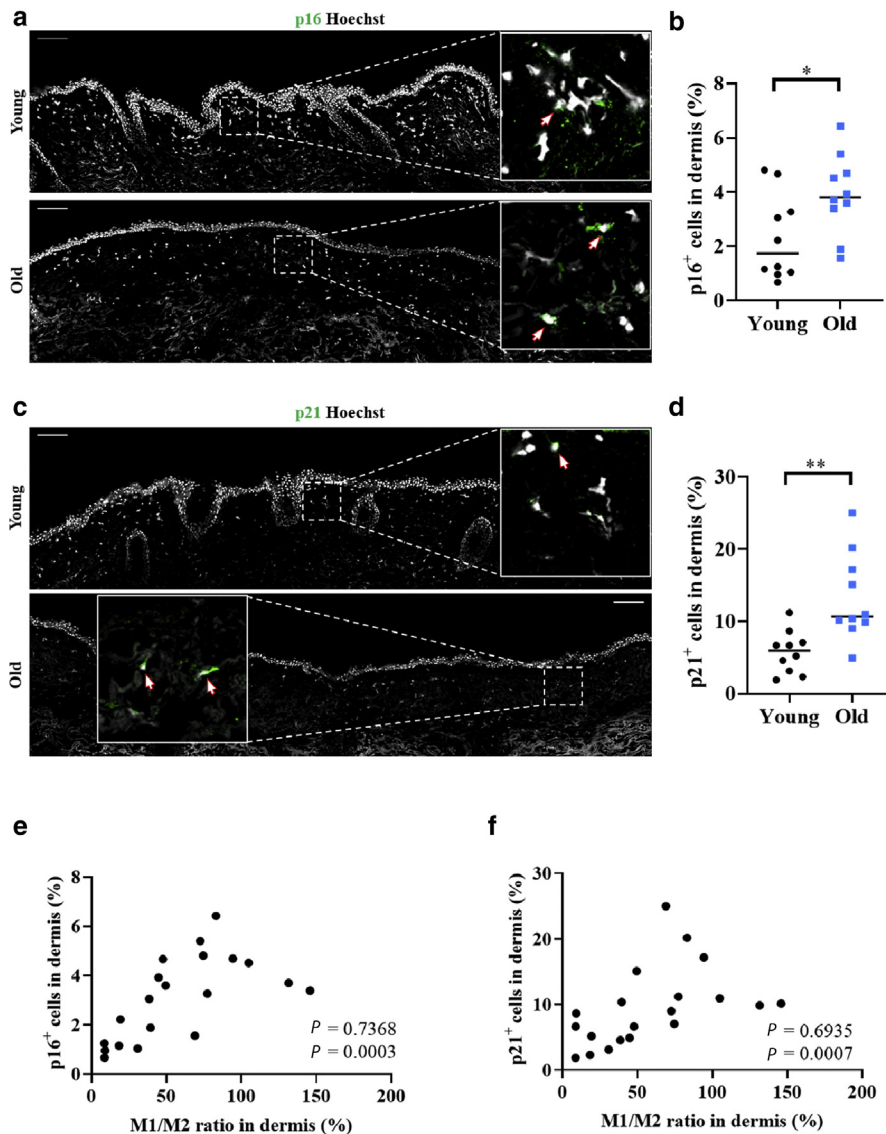
Percentages of dermal p16$^+$ and p21$^+$ cells were significantly increased in sun-exposed aged skin and positively correlated with the M1-to-M2 ratio
We next investigated whether changes in the M1/M2 balance affected the expression of senescence markers in the dermis.

We observed significant increases in the percentages of p16$^+$ cells ($P = 0.0288$, Mann–Whitney U test; Figure 2a and b) and p21$^+$ cells ($P = 0.0019$, Mann–Whitney U test; Figure 2c and d) in aged skin. Interestingly, we also found a significant positive correlation between the percentages of p16$^+$ cells and p21$^+$ cells and the M1-to-M2 ratio in the dermis ($\rho = 0.7368$, $P = 0.0003$ and $\rho = 0.6935$, $P = 0.0007$, Spearman's rank correlation coefficient; Figure 2e and f, respectively), indicating that the M1-to-M2 ratio may affect the percentages of p16$^+$ and p21$^+$ cells in the dermis.

M1 and M2 macrophage phenotypes derived from THP-1 cells
We differentiated THP-1 cells into M0 macrophages and polarized these cells into M1 and M2 macrophages for use in an in vitro assay (Figure 3a). To determine the phenotypes of M1 and M2 macrophages derived from THP-1 cells, we performed real-time RT-PCR and cytokine array analysis and found that M1 and M2 marker expression was similar to that

in previous reports (Figure 3b and c) (Mosser and Edwards, 2008; Parisi et al., 2018). In addition, we confirmed that THP-1–derived M1 macrophages relied on aerobic glycolysis, as indicated by the extracellular acidification rate, whereas THP-1–derived M2 macrophages had an increased mitochondrial oxygen consumption rate (Figure 4a–c), as previously reported (Huang et al., 2014). Therefore, our findings indicate that M1 and M2 macrophages derived from THP-1 cells by our protocol have proinflammatory M1-like and anti-inflammatory M2-like phenotypes, respectively.

M1 macrophages induce senescence in dermal fibroblasts
To investigate whether M1 and M2 macrophages affect dermal fibroblast senescence, we cultured dermal fibroblasts with supernatant from these two macrophage subsets derived from THP-1 cells and peripheral blood monocytes (Figure 5a and b). We examined the effect of the supernatant of M1 and M2 macrophages derived from THP-1 cells. Compared with control medium and M2 macrophage supernatant, M1 macrophage supernatant increased the percentages of SA-β-

gal–positive cells, p21+ cells and p16+ cells (Figure 5c–e and g–i). In addition, compared with the control medium, M2 macrophage supernatant decreased the percentage of SA-β-gal–positive cells (Figure 5c and g). Furthermore, we examined the effect of the supernatant of M1 and M2 macrophages derived from peripheral blood monocytes. Similar to those of THP-1 cells, M1 macrophage supernatant increased the percentages of p16+ cells (Figure 5f and j). These results indicate that M1 macrophage supernatant may have the capacity to induce senescence, whereas M2 macrophage supernatant may have the capacity to inhibit senescence in dermal fibroblasts.

IL-34 inhibits M1 macrophage–induced senescence in dermal fibroblasts
To understand why the M1-to-M2 ratio is altered in sun-exposed aged skin, we analyzed the expression of genes that are known to be involved in macrophage differentiation using the RNA sequencing dataset from the Genotype-Tissue Expression database for skin tissue (https://gtexportal.org/
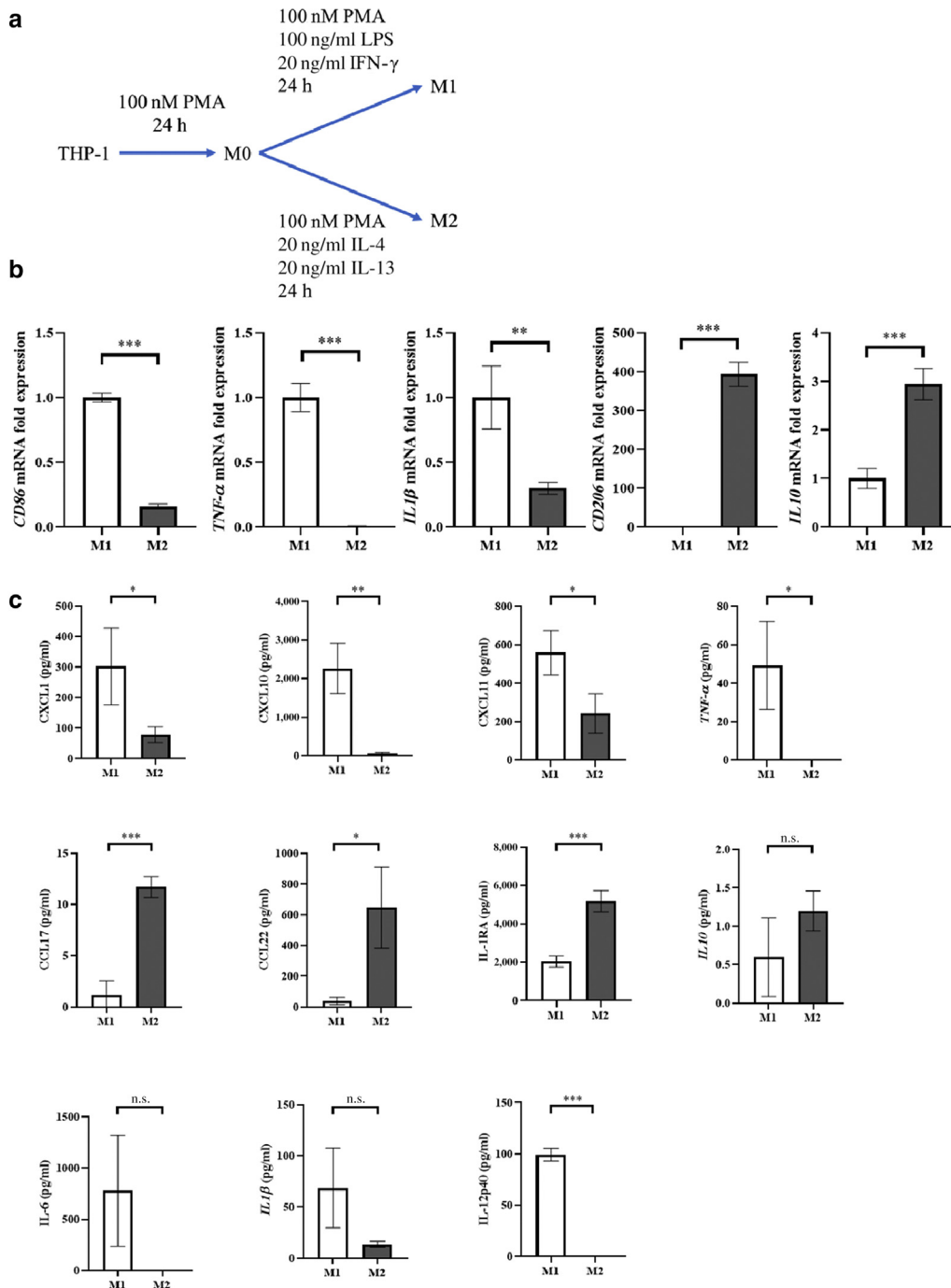
Figure 3. M1 and M2 macrophages derived from THP-1 cells by our protocol have proinflammatory M1-like and anti-inflammatory M2-like phenotypes. (**a**) Experimental scheme for differentiating M0 macrophages and polarizing M0 macrophages to M1 and M2 macrophages. To generate M0 macrophages, THP-1 cells were treated with 100 nM PMA for 24 h. To generate M1 macrophages, M0 macrophages were treated with PMA plus 100 ng/ml LPS and 20 ng/ml IFN-γ for another 24 h. To generate M2 macrophages, M0 macrophages were treated with PMA plus 20 ng/ml IL-4 and 20 ng/ml IL-13 for another 24 h. (**b**) Levels of *CD86* mRNA, *TNF-α* mRNA, *IL1β* mRNA, *CD206* mRNA, and *IL10* mRNA in M1 and M2 macrophages, as measured by real-time RT-PCR. Total RNA was isolated from THP-1 cells using a commercial kit (RNeasy Mini Kit, Qiagen, Chatsworth, CA) according to the manufacturer's instructions. Real-time RT-PCR for *CD86*, *TNF-α*, *IL1β*, *CD206*, *IL10*, and *GAPDH* was performed using a TaqMan RNA-to-C$_T$ 1-Step Kit (Applied Biosystems, Foster City, CA) according to the manufacturer's instructions. Gene-specific probes labeled with fluorescein were purchased from Applied Biosystems. All data are expressed as mean ± SD values. n = 3 for both M1 and M2 macrophages. **$P < 0.01$ and ***$P < 0.001$. (**c**) Levels of CXCL1, CXCL10, CXCL11, TNF-α, CCL17, CCL22, IL-1RA, IL-1β, IL-6, IL-10, and IL-12p40 in the supernatants of M1 and M2 macrophages, as measured by cytokine array analysis. To generate M1 and M2 macrophages, M0 macrophages were stimulated with LPS plus IFN-γ or IL-4 plus IL-13 for 24 h. Then, supernatants were removed and cultured with RPMI-1640 medium (Nacalai Tesque, Kyoto, Japan) supplemented with 0.5% fetal bovine serum and 2 mM L-glutamine at 37 °C for 48 h. Supernatants of M1 and M2 macrophages were harvested and used for the cytokine array analysis. Cytokine profiles were measured with a Quantibody Human Cytokine Antibody Array (RayBiotech, Norcross, GA) according to the manufacturer's instructions. All data are expressed as mean ± SD values. n = 3 for both M1 and M2 macrophages. *$P < 0.05$, **$P < 0.01$, and ***$P < 0.001$. h, hour; LPS, lipopolysaccharide; n.s., not significant; PMA, phorbol 12-myristate 13-acetate.
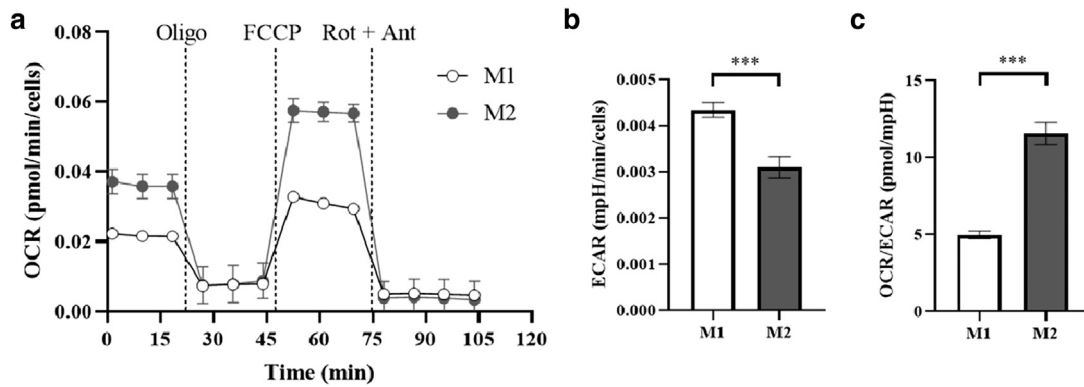
Figure 4. M1 macrophages rely on aerobic glycolysis, measured as the ECAR, whereas M2 macrophages have an increased mitochondrial OCR. (a) Macrophages derived from THP-1 cells were analyzed using an XF Cell Mito Stress Test Kit and an XFe24 EFA (Seahorse Bioscience, North Billerica, MA) for real-time analysis of the ECAR and OCR as described previously (Huang et al., 2014). OCRs in M1 and M2 macrophages were determined using an XF-24 EFA. The following agents were added sequentially: 1 μM oligo, which inhibits mitochondrial ATP synthase; 1 μM FCCP, a protonophore that uncouples ATP synthesis from oxygen consumption through the electron transport chain; and 0.5 μM rot and ant, which inhibit the electron transport chain. Nuclear counterstaining was performed with Hoechst and used for normalization. (**b**) Basal ECARs (changes in mpH per unit time) in M1 and M2 macrophages were measured using the EFA. (**c**) OCR-to-ECAR ratios for M1 and M2 macrophages. All data are expressed as mean ± SD values. n = 4 for both M1 and M2 macrophages. ***$P < 0.001$. Cells were counted after staining with Hoechst. Ant, antimycin A; ATP, adenosine triphosphate; ECAR, extracellular acidification rate; EFA, extracellular flux analyzer; FCCP, fluoro-carbonyl cyanide phenylhydrazone; min, minute; OCR, oxygen consumption rate; oligo, oligomycin; Rot, rotenone.

home/) (Carithers et al., 2015). We found that the expression of several macrophage differentiation–related genes was changed in the sun-exposed skin of subjects in their age 60s compared with that in sun-protected skin (Figure 6a). Among these gene products, we focused on IL-34, which is highly expressed in the skin and is a known inducer of anti-inflammatory macrophages (Baghdadi et al., 2018). We examined the effect of IL-34 on M1 macrophages and found that IL-34 inhibited M1 macrophage–induced senescence in dermal fibroblasts (Figure 6c–f).

IL-34 is downregulated in sun-exposed aged skin and negatively correlates with the M1-to-M2 ratio

Therefore, we focused on IL-34 and further investigated the effect of IL-34 on the M1-to-M2 ratio. We found that the number of IL-34^{+} cells in the epidermis was significantly decreased in sun-exposed aged skin ($P = 0.0449$, Mann–Whitney U test; Figure 7a and b). In addition, we found a negative correlation between the number of IL-34^{+} cells in the epidermis and the M1-to-M2 ratio in the dermis (ρ = 0.4438, $P = 0.0500$, Spearman's rank correlation coefficient; Figure 7e). We also found that the number of cells positive for CSF1R, which is the major IL-34 receptor, was not significantly different between young and aged skin (Figure 7c and d). However, there was a significant positive correlation between the numbers of CD206^{+} CD68^{+} cells and CSF1R^{+} CD68^{+} cells in the dermis (ρ = 0.7600, $P = 0.0001$, Spearman's rank correlation coefficient; Figure 7f). These findings indicate that the increase in the M1-to-M2 ratio in the dermis may be due to a decrease in IL-34 levels and associated downstream signaling.

### IL-34 modulates CD206 and IL-10 expression in macrophages

To examine whether IL-34 regulates macrophage phenotype, we stimulated macrophages derived from human peripheral blood monocytes with IL-34. Although the effect was not significant at 24 hours, we observed a significant positive correlation between the IL-34 dose and the mRNA expression

levels of CD206 after 72 hours ($r = 0.9623$, $P = 0.0087$, Student's t-test for the Pearson correlation coefficient; Figure 7g). In addition to changes in CD206, we observed that IL-10 expression may also be dose-dependently correlated with IL-34 at 72 hours ($r = 0.9470$, $P = 0.0145$, Student's t-test for the Pearson correlation coefficient; Figure 7h). These results indicate that IL-34 may induce an anti-inflammatory phenotype in macrophages and inhibit dermal fibroblast senescence.

DISCUSSION

In this work, we investigated the M1/M2 balance in sun-exposed human skin and the mechanism underlying the changes in the M1/M2 balance with aging. We found that the M1-to-M2 ratio was markedly increased in aged skin and positively correlated with the percentages of p16[+] and p21^{+} senescent cells. Our observations suggest that an increase in the M1-to-M2 ratio correlates with aging in sun-exposed skin. Furthermore, the number of IL-34^{+} cells was reduced in aged skin and negatively correlated with the M1-to-M2 ratio, whereas the number of CSF1R^{+} cells positively correlated with the number of M2 macrophages, suggesting that IL-34 plays a role in regulating the M1/M2 balance.

First, we investigated whether aging affected the M1/M2 balance in sun-exposed skin. We found that the number of M1 macrophages was increased and that of M2 macrophages was significantly decreased; however, the total macrophage count was unchanged, indicating that the M1-to-M2 ratio was markedly increased in aged skin. These results suggest that the differentiation rather than the recruitment of macrophages was changed in aged skin. This is the evidence that the M1/M2 balance in sun-exposed human skin under steady-state conditions is increased in elderly individuals. In this study, we divided macrophages into two subsets: M1 and M2. However, previous reports have shown that macrophage subtypes are much more complex in vivo and that macrophage subclassification is important when investigating their role in tissue
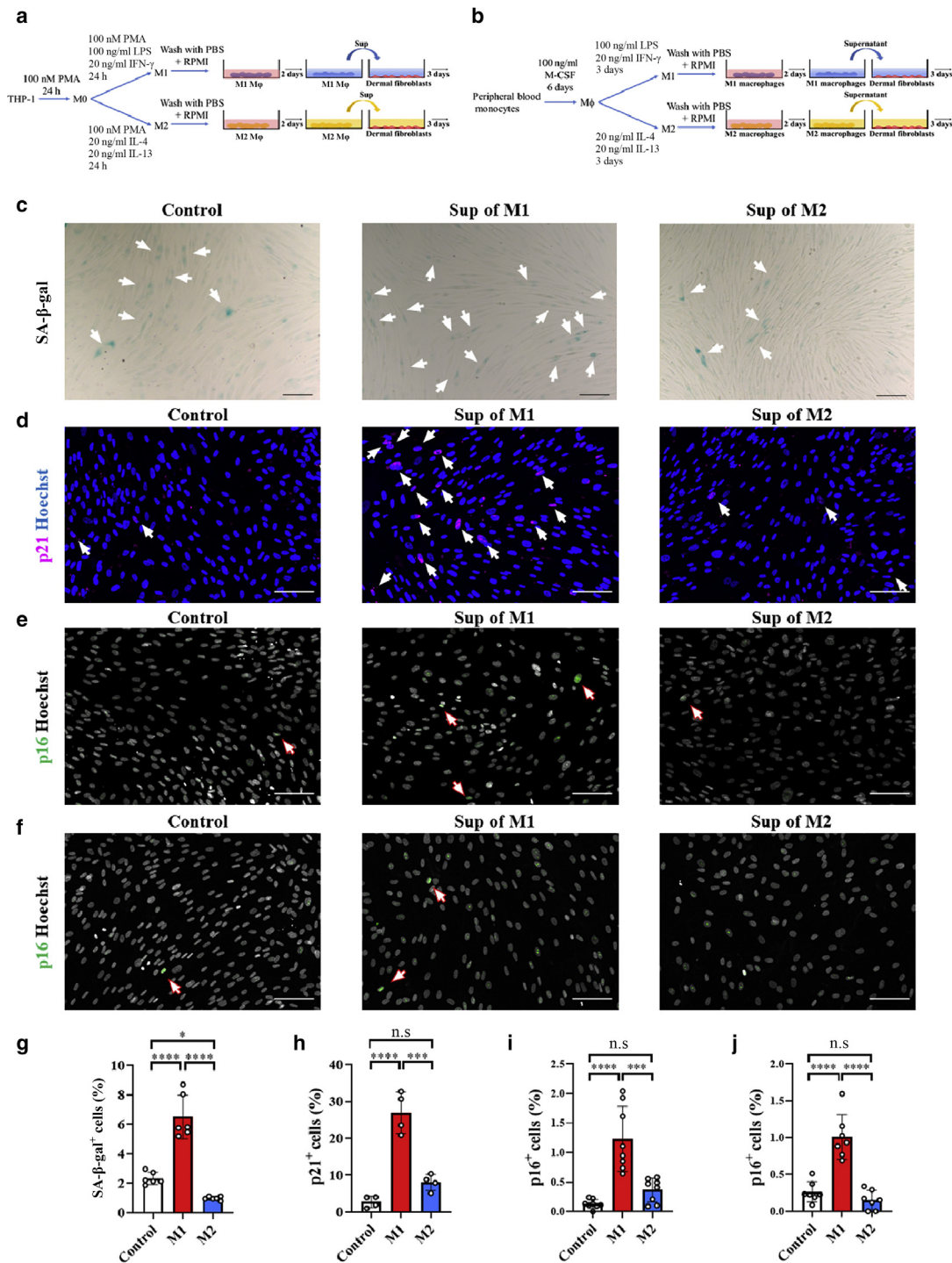
Figure 5. M1 Mφs derived from THP-1 cells increased p21 expression and SA-β-gal activity in dermal fibroblasts in vitro. (a, b) Experimental scheme for examining the effect of Sups from M1 and M2 Mφs on dermal fibroblasts in vitro. (c) Representative SA-β-gal–stained (blue, a marker of senescent cells) dermal fibroblasts. The arrows indicate SA-β-gal$^+$ dermal fibroblasts. (d) Representative p21 (magenta) immunofluorescence-stained dermal fibroblasts. The arrows indicate p21$^+$ dermal fibroblasts. Nuclei were stained with Hoechst (blue). (e) Representative p16 (green) immunofluorescence-stained dermal fibroblasts that were added to the Sup of Mφs derived from THP-1 cells. The arrows indicate p16$^+$ dermal fibroblasts. Nuclei were stained with Hoechst (gray). (f) Representative p16 (green) immunofluorescence-stained dermal fibroblasts that were added to the Sup of Mφs derived from peripheral blood monocytes. The arrows indicate p16$^+$ dermal fibroblasts. Nuclei were stained with Hoechst (gray). (g) Quantitation of the percentage of SA-β-gal$^+$ dermal fibroblasts. (h) Quantitation of the percentage of p21$^+$ dermal fibroblasts. (i) Quantitation of the percentage of p16$^+$ dermal fibroblasts that were added to the Sup of Mφs derived from THP-1 cells. (j) Quantitation of the percentage of p16$^+$ dermal fibroblasts that were added to the Sup of Mφs derived from peripheral blood monocytes. All data are expressed as mean ± SD values. n = 4–8 for control and M1 and M2 macrophages. *$P < 0.05$, ***$P < 0.001$, and ****$P < 0.0001$. To test for significance, Tukey's multiple comparisons test was utilized. Bar = 100 μm. h, hour; LPS, lipopolysaccharide; Mφ, macrophage; n.s., not significant; PMA, phorbol 12-myristate 13-acetate; SA-β-gal, senescence-associated β-galactosidase; Sup, supernatant.
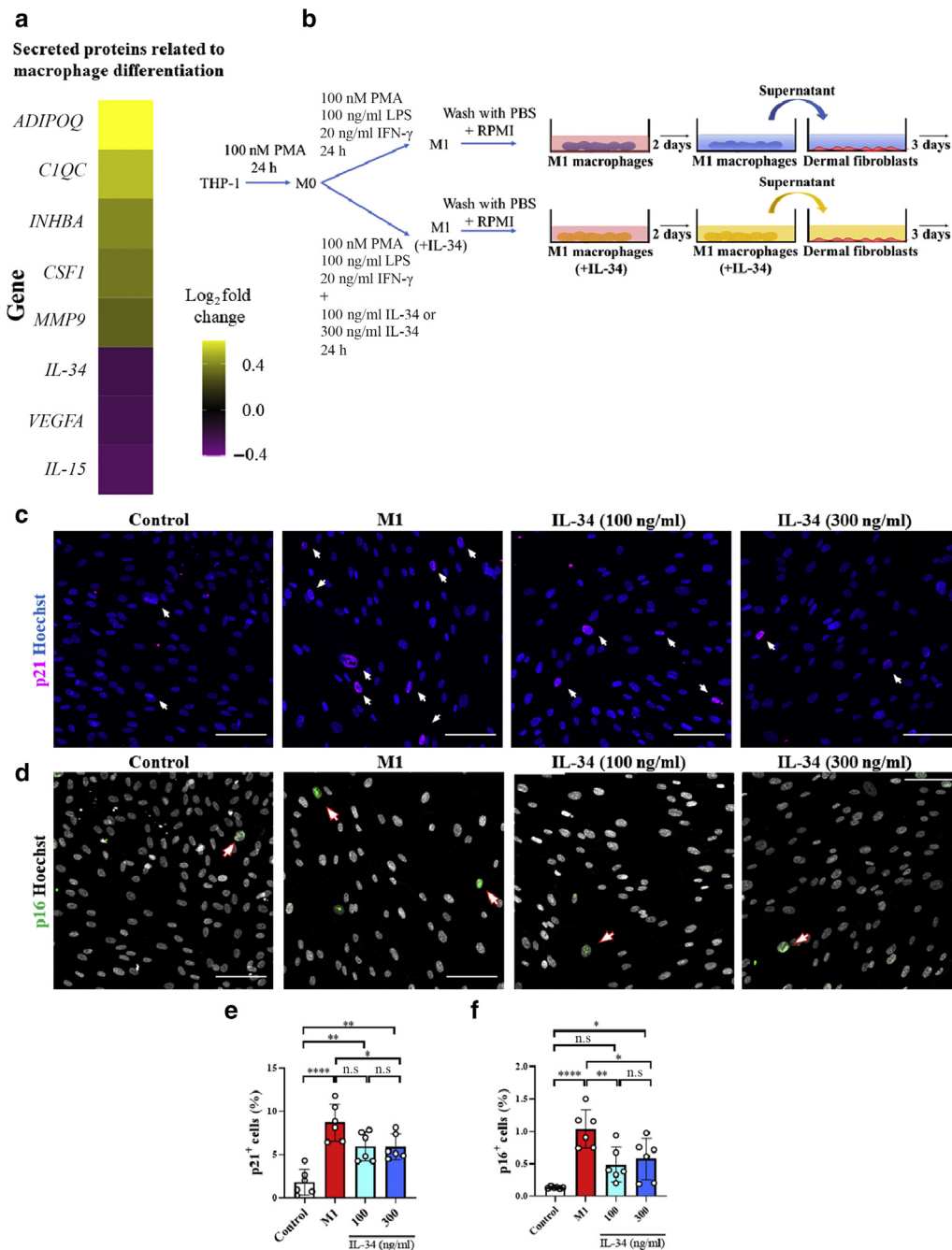
Figure 6. IL-34 inhibited the senescence-inducing effect of M1 macrophages on dermal fibroblasts. (**a**) The expression profiles of genes involved in macrophage differentiation (GO:0030225, GO:0045650, and GO:0045651) using the RNA-seq dataset from the GTEx (version 8) database for skin tissue. Fold change between sun-exposed skin and sun-protected skin of subjects in their age 60s was calculated. The genes for which FDR < 0.05 are shown. (**b**) Experimental scheme for examining the effect of supernatants from M1 and M1 macrophages polarized with IL-34 on dermal fibroblasts in vitro. (**c**) Representative p21 (magenta) immunofluorescence-stained dermal fibroblasts. The arrows indicate p21$^+$ dermal fibroblasts. Nuclei were stained with Hoechst (blue). (**d**) Representative p16 (green) immunofluorescence-stained dermal fibroblasts. The arrows indicate p16$^+$ dermal fibroblasts. Nuclei were stained with Hoechst (gray). (**e**) Quantitation of the percentage of p21$^+$ dermal fibroblasts. (**f**) Quantitation of the percentage of p16$^+$ dermal fibroblasts. All data are expressed as mean ± SD values. n = 6. *P < 0.05, **P < 0.01, and ****P < 0.0001. To test for significance, Tukey's multiple comparisons test was utilized. Bar = 100 μm. FDR, false recovery rate; GO, Gene Ontology; GTEx, Genotype-Tissue Expression; h, hour; LPS, lipopolysaccharide; n.s., not significant; PMA, phorbol 12-myristate 13-acetate; RNA-seq, RNA sequencing.

homeostasis or disease (Satoh et al., 2013). To further elucidate the relationship between skin aging and the M1-to-M2 ratio in humans, it will be necessary to identify the subtypes of M1 and M2 macrophages with altered numbers in elderly individuals.

Next, we investigated whether M1 or M2 macrophages influence aging in sun-exposed skin, and we found a positive correlation between the M1-to-M2 ratio and the percentages of p16$^+$ and p21$^+$ senescent cells. In addition, we found that proinflammatory M1 macrophages were increased in aged skin and that THP-1–derived M1 macrophages induced p21 and p16 expression and SA-β-gal activity. It has been reported that inflammatory mechanisms may accentuate the effect of UVR and amplify aging (Bennett et al., 2008), and aged sun-exposed skin displays histological features of

chronic inflammation (Bosset et al., 2003). In addition, a previous report revealed that M1 macrophages are associated with the induction of inflammatory response genes and that CD86 expression is elevated on macrophages that are associated with chronic inflammation (Xue et al., 2014). Our results, together with the reported findings, suggest that a proinflammatory milieu induced by increased M1 macrophages in aged skin accelerates aging in sun-exposed skin.

On the contrary, M2 macrophages can produce anti-inflammatory cytokines and play a key role in clearing debris or dying cells through a process called efferocytosis, which is a critical step in the resolution of inflammation (Gilroy and De Maeyer, 2015; Pattabiraman et al., 2017). We found that the number of M2 macrophages was significantly

Figure 7. IL-34 was downregulated in old skin and negatively correlated with the M1-to-M2 ratio. (a) Representative IL-34 (green) immunofluorescence-stained samples of young and old human skin. Nuclei were stained with Hoechst (gray). (b) Quantitation of IL-34$^+$ cells in the epidermis. (c) Representative CSF1R (green) and CD68 (red) immunofluorescence-stained samples of young and old human skin. The arrows indicate CSF1R$^+$ CD68$^+$ cells in the dermis. Nuclei were stained with Hoechst (blue). (d) Quantitation of CSF1R$^+$ CD68$^+$ cells/mm^2 in the dermis. (e) Correlation between IL-34$^+$ cells in the epidermis and the M1-to-M2 ratio in the dermis for young and old skin samples. (f) Correlation between CD206$^+$ CD68$^+$ cells in the dermis and CSF1R$^+$ CD68$^+$ cells in the dermis for young and old skin samples. (g) Levels of *CD206* mRNA in macrophages differentiated from human peripheral blood monocytes after stimulation with IL-34 for 24 or 72 h, as measured by real-time RT-PCR. (h) Levels of *IL10* mRNA in macrophages differentiated from human peripheral blood monocytes after stimulation with IL-34 for 24 or 72 h, as measured by real-time RT-PCR. To test for significance, Student's *t*-test for the Pearson correlation coefficient was utilized. $P < 0.05$ was considered to indicate a significant difference. All data are expressed as mean ± SD values. n = 10 in both the young and old groups. *$P < 0.05$. To test for significance for young and old skin, Mann–Whitney U test was utilized. To test for the significance of scatter plots, Spearman's rank correlation coefficient was utilized. Bar = 100 μm. h, hour; n.s., not significant.
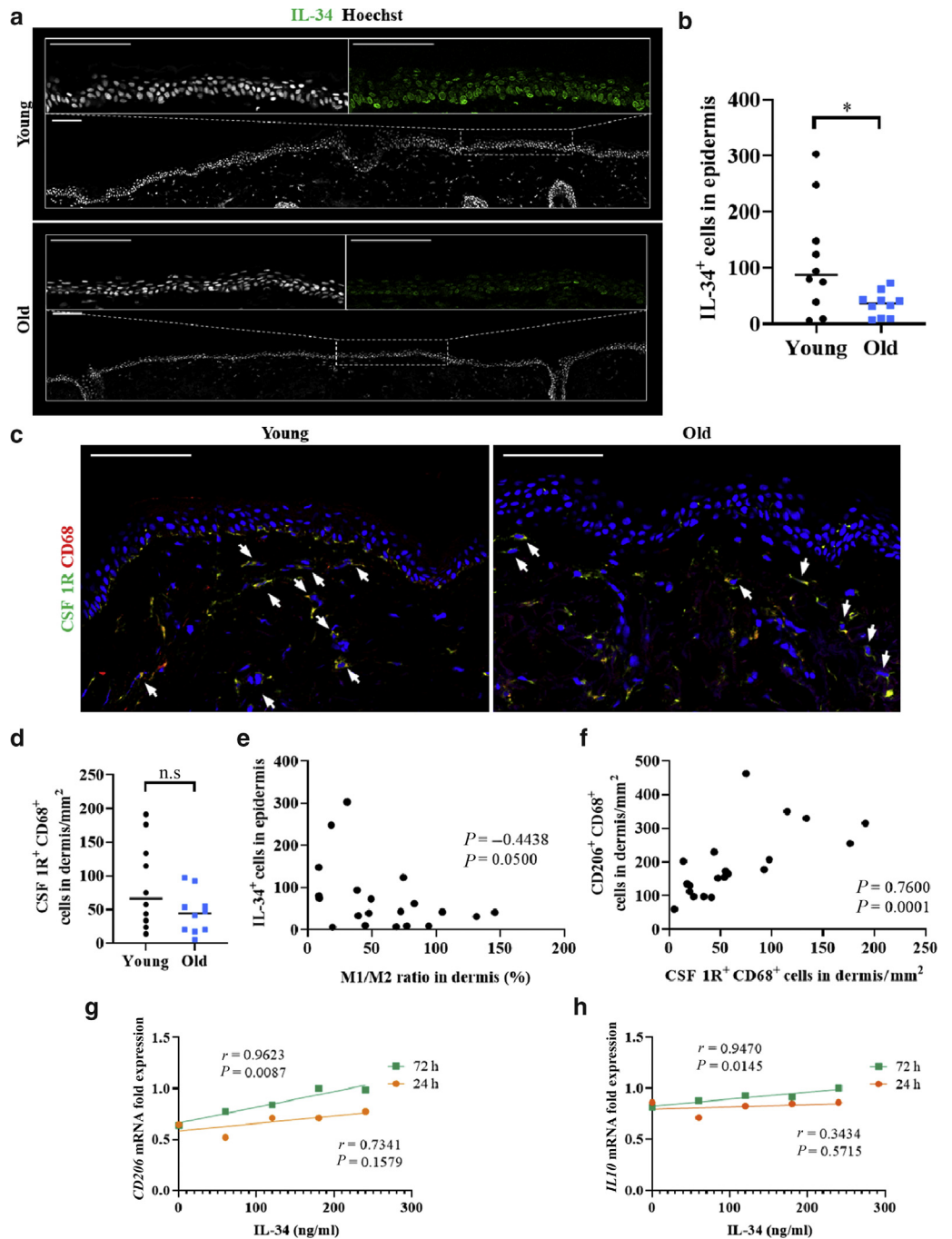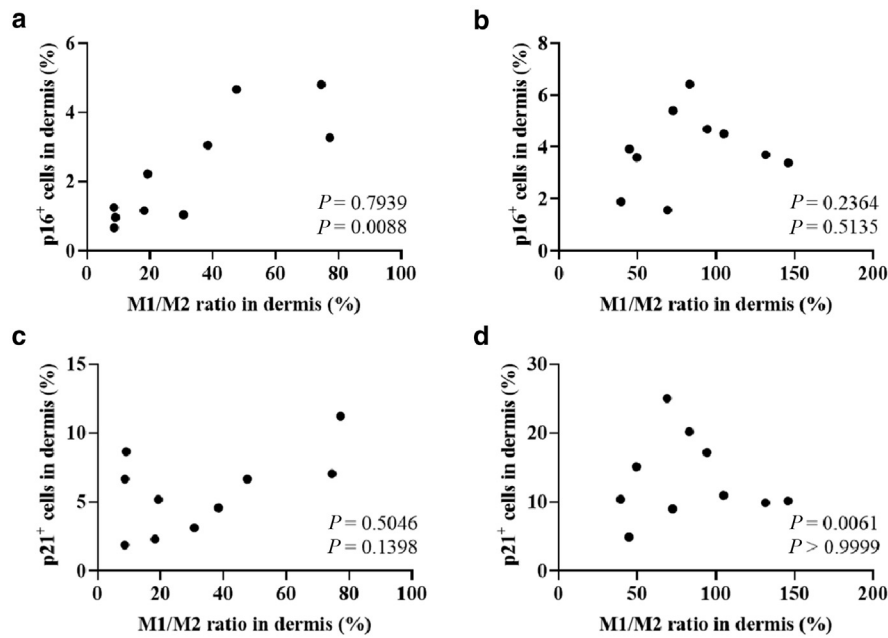

decreased in aged skin and that THP-1–derived M2 macrophages inhibited SA-β-gal activity, suggesting that this decrease may also affect chronic inflammation and aging. Alterations in macrophage phenotype and function drive aging through a process associated with a state of low-grade, chronic inflammation, which is known as inflammaging (De Maeyer et al., 2020; van Beek et al., 2019). Our findings suggest that an increase in the M1-to-M2 ratio resulting from both an increase in M1 macrophages and a decrease in M2 macrophages accelerates inflammaging in elderly sun-exposed skin.

In this study, although the total number of macrophages was not changed, we found that anti-inflammatory M2 macrophages were significantly reduced in sun-exposed aged skin, suggesting that the anti-inflammatory milieu may be impaired with aging in sun-exposed skin. Therefore, to understand the mechanism of inflammaging in sun-exposed skin, we investigated the factors that control M2 macrophage polarization. Our analysis of a dataset from the Genotype-Tissue Expression database showed the downregulation of IL-34 in the sun-exposed skin of subjects in their age 60s compared with that in sun-protected skin, suggesting the involvement of the IL-34 pathway in macrophage differentiation and inflammaging in sun-exposed aged skin. IL-34 is a ligand of CSF1R and shows tissue-specific expression in

organs such as the brain and skin. IL-34 is exclusively expressed by keratinocytes in the epidermis, has a higher affinity for CSF1R than CSF1, and plays a role in promoting the development of Langerhans cells (Baghdadi et al., 2018; Wang and Colonna, 2014). In addition, previous reports indicate that CSF1 and IL-34 exhibit different abilities to polarize macrophages and that IL-34 induces macrophage polarization to an immunosuppressive phenotype (Boulakirba et al., 2018; Foucher et al., 2013; Liu et al., 2019). However, the effects of IL-34 on the M1-to-M2 ratio and inflammaging in the skin are still poorly understood. Therefore, we focused on the cytokine IL-34 and analyzed the mechanism of the skewed M1/M2 balance in sun-exposed aged skin. We found that the number of IL-34$^+$ cells was significantly decreased in the epidermis in sun-exposed aged skin. In addition, the number of IL-34$^+$ cells in the epidermis was negatively correlated with the M1-to-M2 ratio, suggesting that IL-34 derived from the epidermis decreased the M1-to-M2 ratio and may ameliorate inflammaging. Furthermore, the number of CSF1R$^+$ cells in the dermis was positively correlated with the number of M2 macrophages. These results suggest that as CSF1R expression increases, macrophages receive increasing amounts of IL-34 and become polarized to the M2 phenotype in the dermis; moreover, these results indicate that IL-34 may ameliorate inflammaging. To determine whether IL-34 affects the polarization of M2 macrophages, we performed an in vitro assay. We found that IL-34 dose-dependently induced the expression of CD206 and IL-10 in macrophages derived from peripheral monocytes. IL-10 is an M2-associated anti-inflammatory cytokine (Shapouri-Moghaddam et al., 2018), and these results suggest that IL-34 modulates the M1-to-M2 ratio by inducing M2 macrophage polarization and an anti-inflammatory milieu in sun-exposed skin. Previous reports have shown that cells undergoing senescence secrete inflammatory factors, which is referred to as the senescence-associated secretory phenotype. These factors from senescent dermal fibroblasts attract inflammatory immune cells and induce inflammaging in sun-protected skin (Pilkington et al., 2020; van Deursen, 2014). In this study, we found that young skin showed a stronger relationship between the M1-to-M2 ratio and the percentages of p16$^+$ or p21$^+$ cells than aged skin, which expresses more senescence-associated secretory phenotype factors (Figure 8), suggesting that inflammaging is induced not only by the inflammatory skin milieu associated with senescence-associated secretory phenotype, as has been reported, but also by the downregulation of a specific anti-inflammatory pathway mediated by IL-34 downregulation in sun-exposed skin. Indeed, it has been reported that it is important to modify the pathways that initiate resolution processes, including efferocytosis, by M2-like macrophages to treat chronic inflammatory pathology (Fullerton and Gilroy, 2016). Interestingly, IL-34 shows tissue-specific expression in the skin and is downregulated in sun-exposed skin of individuals in their age 60s, and a previous report indicated that the expression of IL-34 in sun-protected skin does not change with aging, suggesting that the IL-34 downregulation–mediated increase in the M1-to-M2 ratio with aging may be a specific pathway in the skin, especially in sun-exposed areas (Baghdadi et al., 2018; Carithers et al., 2015; Hasegawa et al., 2020). Therefore, aging-related downregulation of IL-34 in keratinocytes may explain the increase in the M1-to-M2 ratio and constitutes a possible mechanism underlying the accelerated inflammaging of sun-exposed skin. Thus, enhancing IL-34 expression with agents such as vitamin D, which is known to upregulate the expression of IL-34 in keratinocytes, may ameliorate M1/M2 balance–related inflammaging in sun-exposed skin. Indeed, vitamin D is recognized as an effective skin-protective substance that prevents aging in sun-exposed skin (Bi et al., 2019). Although our results indicate that aging-related IL-34 downregulation may control the M1-to-M2 ratio, the precise

mechanism by which the expression of IL-34 is altered with aging and the mechanism through which anti-inflammatory macrophages or IL-10 inhibit senescence in the dermis require further investigation. In addition, although IL-34 induced anti-inflammatory macrophage polarization at 72 hours, the effect was not strong and was not apparent at 24 hours. To investigate the mechanisms in further detail, we need to develop an ex vivo skin model that can be cultured for a longer time and is more similar to human skin than currently available models. This strategy may provide insight into how homeostasis is maintained in sun-exposed skin.

In summary, although chronic inflammation accelerates the aging of sun-exposed skin, the underlying mechanism is not fully understood. In this study, we show that alterations in the M1-to-M2 ratio in sun-exposed skin contribute to inflammaging and that the M1-to-M2 ratio represents a potential therapeutic target for preventing this process. These findings shed light on the pathophysiology of sun-exposed skin.

MATERIALS AND METHODS
Human skin tissue study
Normal face skin samples, obtained from Caucasian young female cadavers (aged 25–43 years, mean age = 34.2 years) and old female cadavers (aged 62–88 years, mean age = 74.5 years), were kindly provided by Obio (El Segundo, CA) and complied with all applicable laws and rules, ethical codes, and regulations. In addition, they were obtained with informed consent in compliance with all the regulations by the supplier. During the experiments, all samples were identified with randomly assigned codes. It was confirmed before the study that Obio had obtained written informed consent. The use of human skin samples was also approved by the Ethics Committee of Shiseido Global Innovation Center (S/PARK) (Yokohama, Japan).

Immunofluorescence staining of human skin tissues
After isolation, human skin samples were immediately embedded in an optimal cutting temperature compound (Sakura Finetek, Tokyo, Japan), frozen in liquid nitrogen, and stored at −80 °C. Ten-micrometer sections were cut with a microtome, blocked with protein blocking solution (X0909, Dako, Glostrup, Denmark), and incubated overnight at 4 °C with primary antibodies against CD11b (1:100; 49420, Cell Signaling Technology, Danvers, MA), CD206 (1:200; AF2534, R&D Systems, Minneapolis, MN), CD68 (1:100; ab955, Abcam, Cambridge, United Kingdom), CD86 (1:50; AF141NA, R&D Systems), CSF1R (1:100; ab183316, Abcam), IL-34 (1:100; ab101443, Abcam), p16 (1:100; ab108349, Abcam), or p21 (1:100; ab109520, Abcam). The sections were then incubated with corresponding secondary antibodies labeled with Alexa Fluor 488, 594, and 647. Nuclear counterstaining was performed with Hoechst. Stained tissues were imaged with a Zeiss confocal microscope (LSM-880) (Carl Zeiss, Oberkochen, Germany). In the dermis, positive cells located within 200 μm of the epidermal border were evaluated. For each sample, images from >5 high-power fields (×200 magnification) in total were assessed. Positive cells (cells/mm^2) were calculated by counting the positive cells in total fields (>5 fields) and divided by the gross area.

Cell preparations
THP-1 cells were obtained from ATCC (Manassas, VA), and human peripheral blood monocytes (HC-0002) were obtained from Lifeline Cell Technology (Frederick, MD). They were cultured in RPMI-1640

medium (Nacalai Tesque, Kyoto, Japan) supplemented with 10% fetal bovine serum, 1 mM sodium pyruvate, and 2 mM L-glutamine at 37 °C. They were differentiated into M0, M1, and M2 macrophages using a standard protocol described previously (Tjiu et al., 2009). Normal human newborn dermal fibroblasts (Kurabo Industries, Osaka, Japan) were cultured in DMEM (Invitrogen, Carlsbad, CA) supplemented with 10% fetal bovine serum, 100 units/ml penicillin, and 100 μg/ml streptomycin at 37 °C. To determine the effect of IL-34, macrophages differentiated from human peripheral blood monocytes were treated with IL-34 for 24 hours or 72 hours.

Real-time RT-PCR
Total RNA was isolated from THP-1 cells or peripheral blood monocytes using a commercial kit (RNeasy Mini Kit, Qiagen, Chatsworth, CA) according to the manufacturer's instructions. Real-time RT-PCR for *CD206*, *IL10*, and *GAPDH* was performed using a TaqMan RNA-to C$_T$ 1-Step Kit (Applied Biosystems, Foster City, CA) according to the manufacturer's instructions. Gene-specific probes labeled with fluorescein were purchased from Applied Biosystems.

Immunostaining of p21 and p16 and detection of SA-β-gal activity
Normal human newborn foreskin dermal fibroblasts (Kurabo Industries) were seeded at a density of 0.6×10^5 cells/well into four-well culture slides (Corning, Corning, NY). M1 and M2 macrophages derived from THP-1 cells and peripheral blood monocytes were cultured with RPMI-1640 medium supplemented with 0.5% fetal bovine serum, 500 μM ascorbic acid, and 2 mM L-glutamine at 37 °C for 48 hours, and the supernatants of these cells were then added to the dermal fibroblasts. As the control, dermal fibroblasts were incubated for 3 days in RPMI-1640 medium supplemented with 0.5% fetal bovine serum, 500 μM ascorbic acid, and 2 mM L-glutamine. At 72 hours after application of the supernatants of M1 or M2 macrophages, SA-β-gal activity was detected using a Senescence Detection Kit (ab65351, Abcam) according to the manufacturer's instructions. To count p21$^+$ and p16$^+$ cells, cells were incubated overnight at 4 °C with an antibody against p21 (1:100; ab109520, Abcam) and p16 (1:200; ab108349, Abcam) and then with a corresponding secondary antibody labeled with Alexa Fluor 488 and 568. Nuclear counterstaining was performed with Hoechst.

RNA sequencing data analysis
The RNA sequencing dataset was obtained from the Genotype-Tissue Expression portal (https://gtexportal.org/home/). In this experiment, we used processed Trusted Platform Module data of healthy individuals. Genotype-Tissue Expression, version 8, contains data for 232 sun-exposed skin (lower leg) and 202 sun-protected skin (suprapubic) samples of individuals in their age 60s. To extract the genes involved in macrophage differentiation, we used Gene Ontology terms related to macrophage differentiation (Gene Ontology: 0030225, Gene Ontology: 0045650, and Gene Ontology: 0045651). Because the dataset is partially paired, we employed an optimal pooled *t*-test (Guo and Yuan, 2017) using R. *P*-values were adjusted for false discovery rate.

Statistical analysis
Data were analyzed using GraphPad Prism (GraphPad Software, San Diego, CA). Column scatter plots show the mean value ± SD. To compare cell counts in the skin, the Mann–Whitney U test was utilized. To compare counts of SA-β-gal–positive cells and percentages of p21- and p16-positive cells, mRNA expression, cytokine expression, oxygen consumption rate, and extracellular acidification

rate, Student's *t*-test, the Mann-Whitney U test, or Tukey's multiple comparisons test was utilized. For scatter plots, Student's *t*-test for the Pearson correlation coefficient or Spearman's rank correlation coefficient was utilized. $P < 0.05$ was considered to indicate a significant difference.

Data availability statement
The data supporting the findings of this study are available from the corresponding author on reasonable request.

ORCIDs
Satoshi Horiba: http://orcid.org/0000-0002-7047-0097
Ryota Kami: http://orcid.org/0000-0001-5052-6068
Taiki Tsutsui: http://orcid.org/0000-0002-9793-4402
Junichi Hosoi: http://orcid.org/0000-0002-8534-9652

REFERENCES

Akiyama K, Chen C, Wang D, Xu X, Qu C, Yamaza T, et al. Mesenchymal-stem-cell-induced immunoregulation involves FAS-ligand-/FAS-mediated T cell apoptosis. Cell Stem Cell 2012;10:544–55.

Baghdadi M, Umeyama Y, Hama N, Kobayashi T, Han N, Wada H, et al. Interleukin-34, a comprehensive review. J Leukoc Biol 2018;104:931–51.

Bennett MF, Robinson MK, Baron ED, Cooper KD. Skin immune systems and inflammation: protector of the skin or promoter of aging? J Investig Dermatol Symp Proc 2008;13:15–9.

Bi Y, Xia H, Li L, Lee RJ, Xie J, Liu Z, et al. Liposomal vitamin D3 as an anti-aging agent for the skin. Pharmaceutics 2019;11:311.

Bosset S, Bonnet-Duquennoy M, Barré P, Chalon A, Kurfurst R, Bonté F, et al. Photoageing shows histological features of chronic skin inflammation without clinical and molecular abnormalities. Br J Dermatol 2003;149: 826–35.

Boulakirba S, Pfeifer A, Mhaidly R, Obba S, Goulard M, Schmitt T, et al. IL-34 and CSF-1 display an equivalent macrophage differentiation ability but a different polarization potential. Sci Rep 2018;8:256.

Carithers LJ, Ardlie K, Barcus M, Branton PA, Britton A, Buia SA, et al. A novel approach to high-quality postmortem tissue procurement: the GTEx project. Biopreserv Biobank 2015;13:311–9.

Chen W, Kang J, Xia J, Li Y, Yang B, Chen B, et al. p53-related apoptosis resistance and tumor suppression activity in UVB-induced premature senescent human skin fibroblasts. Int J Mol Med 2008;21:645–53.

De Maeyer RPH, van de Merwe RC, Louie R, Bracken OV, Devine OP, Goldstein DR, et al. Blocking elevated p38 MAPK restores efferocytosis and inflammatory resolution in the elderly [published correction appears in Nat Immunol 2020;21:696]. Nat Immunol 2020;21:615–25.

Eapen MS, Hansbro PM, McAlinden K, Kim RY, Ward C, Hackett TL, et al. Abnormal M1/M2 macrophage phenotype profiles in the small airway wall and lumen in smokers and chronic obstructive pulmonary disease (COPD). Sci Rep 2017;7:13392.

Fisher GJ, Kang S, Varani J, Bata-Csorgo Z, Wan Y, Datta S, et al. Mechanisms of photoaging and chronological skin aging. Arch Dermatol 2002;138: 1462–70.

Foucher ED, Blanchard S, Preisser L, Garo E, Ifrah N, Guardiola P, et al. IL-34 induces the differentiation of human monocytes into immunosuppressive macrophages. antagonistic effects of GM-CSF and IFNγ [published correction appears in PLoS One 2014;9]. PLoS One 2013;8:e56045.

Fullerton JN, Gilroy DW. Resolution of inflammation: a new therapeutic frontier. Nat Rev Drug Discov 2016;15:551–67.

Gilroy D, De Maeyer R. New insights into the resolution of inflammation. Semin Immunol 2015;27:161–8.

Gordon JR, Brieva JC. Images in clinical medicine. Unilateral dermatoheliosis. N Engl J Med 2012;366:e25.

Guo B, Yuan Y. A comparative review of methods for comparing means using partially paired data. Stat Methods Med Res 2017;26:1323–40.

Hasegawa T, Feng Z, Yan Z, Ngo KH, Hosoi J, Demehri S. Reduction in human epidermal Langerhans cells with age is associated with decline in CXCL14-mediated recruitment of CD14$^+$ monocytes. J Invest Dermatol 2020;140:1327–34.

Huang SC, Everts B, Ivanova Y, O'Sullivan D, Nascimento M, Smith AM, et al. Cell-intrinsic lysosomal lipolysis is essential for alternative activation of macrophages. Nat Immunol 2014;15:846–55.

Idda ML, McClusky WG, Lodde V, Munk R, Abdelmohsen K, Rossi M, et al. Survey of senescent cell markers with age in human tissues. Aging (Albany NY) 2020;12:4052–66.

Liu Y, Liu H, Zhu J, Bian Z. Interleukin-34 drives macrophage polarization to the M2 phenotype in autoimmune hepatitis. Pathol Res Pract 2019;215: 152493.

Lucas T, Waisman A, Ranjan R, Roes J, Krieg T, Müller W, et al. Differential roles of macrophages in diverse phases of skin repair. J Immunol 2010;184:3964–77.

Martinez FO, Gordon S. The M1 and M2 paradigm of macrophage activation: time for reassessment. F1000Prime Rep 2014;6:13.

Mescher AL. Macrophages and fibroblasts during inflammation and tissue repair in models of organ regeneration. Regeneration (Oxf) 2017;4: 39–53.

Mosser DM, Edwards JP. Exploring the full spectrum of macrophage activation [published correction appears in Nat Rev Immunol 2010;10:460]. Nat Rev Immunol 2008;8:958–69.

Mowat AM, Scott CL, Bain CC. Barrier-tissue macrophages: functional adaptation to environmental challenges. Nat Med 2017;23:1258–70.

Natsuaki Y, Egawa G, Nakamizo S, Ono S, Hanakawa S, Okada T, et al. Perivascular leukocyte clusters are essential for efficient activation of effector T cells in the skin. Nat Immunol 2014;15:1064–9.

Parisi L, Gini E, Baci D, Tremolati M, Fanuli M, Bassani B, et al. Macrophage polarization in chronic inflammatory diseases: killers or builders? J Immunol Res 2018;2018:8917804.

Pattabiraman G, Palasiewicz K, Galvin JP, Ucker DS. Aging-associated dysregulation of homeostatic immune response termination (and not initiation). Aging Cell 2017;16:585–93.

Pilkington SM, Bulfone-Paus S, Griffiths CEM, Watson REB. Inflammaging and the skin. J Invest Dermatol 2021;141:1087–95.

Qin Z, Okubo T, Voorhees JJ, Fisher GJ, Quan T. Elevated cysteine-rich protein 61 (CCN1) promotes skin aging via upregulation of IL-1β in chronically sun-exposed human skin. Age (Dordr) 2014;36:353–64.

Ressler S, Bartkova J, Niederegger H, Bartek J, Scharffetter-Kochanek K, Jansen-Dürr P, et al. p16INK4A is a robust in vivo biomarker of cellular aging in human skin. Aging Cell 2006;5:379–89.

Rittié L, Fisher GJ. Natural and sun-induced aging of human skin. Cold Spring Harb Perspect Med 2015;5:a015370.

Satoh T, Kidoya H, Naito H, Yamamoto M, Takemura N, Nakagawa K, et al. Critical role of Trib1 in differentiation of tissue-resident M2-like macrophages. Nature 2013;495:524–8.

Shapouri-Moghaddam A, Mohammadian S, Vazini H, Taghadosi M, Esmaeili SA, Mardani F, et al. Macrophage plasticity, polarization, and function in health and disease. J Cell Physiol 2018;233:6425–40.

Shook BA, Wasko RR, Rivera-Gonzalez GC, Salazar-Gatzimas E, López-Giráldez F, Dash BC, et al. Myofibroblast proliferation and heterogeneity are supported by macrophages during skin repair. Science 2018;362: eaar2971.

Tjiu JW, Chen JS, Shun CT, Lin SJ, Liao YH, Chu CY, et al. Tumor-associated macrophage-induced invasion and angiogenesis of human basal cell carcinoma cells by cyclooxygenase-2 induction [published correction appear in J Invest Dermatol 2018;138:471]. J Invest Dermatol 2009;129: 1016−25.

Tsepkolenko A, Tsepkolenko V, Dash S, Mishra A, Bader A, Melerzanov A, et al. The regenerative potential of skin and the immune system. Clin Cosmet Investig Dermatol 2019;12:519−32.

van Beek AA, Van den Bossche J, Mastroberardino PG, de Winther MPJ, Leenen PJM. Metabolic alterations in aging macrophages: ingredients for inflammaging? Trends Immunol 2019;40:113−27.

van Deursen JM. The role of senescent cells in ageing. Nature 2014;509: 439−46.

Wang Y, Colonna M. Interkeukin-34, a cytokine crucial for the differentiation and maintenance of tissue resident macrophages and Langerhans cells. Eur J Immunol 2014;44:1575−81.

Wynn TA, Vannella KM. Macrophages in tissue repair, regeneration, and fibrosis. Immunity 2016;44:450−62.

Xue J, Schmidt SV, Sander J, Draffehn A, Krebs W, Quester I, et al. Transcriptome-based network analysis reveals a spectrum model of human macrophage activation. Immunity 2014;40:274−88.

Yanez DA, Lacher RK, Vidyarthi A, Colegio OR. The role of macrophages in skin homeostasis. Pflugers Arch 2017;469:455−63.

Yoshida H, Okada Y. Role of HYBID (hyaluronan binding protein involved in hyaluronan depolymerization), alias KIAA1199/CEMIP, in hyaluronan degradation in normal and photoaged skin. Int J Mol Sci 2019;20:5804.